# How Efficient is Rotational Mixing in Massive Stars ?

I. Brott*, I. Hunter†, P. Anders* and N. Langer*

*Sterrenkundig Instituut Utrecht, Princetonplein 5, 3584 CC Utrecht, The Netherlands
†Department of Physics and Astronomy, The Queen's University of Belfast, BT7 1NN, Northern Ireland, UK

**Abstract.** The VLT-Flames Survey for Massive Stars [1, 2] provides precise measurements of rotational velocities and nitrogen surface abundances of massive stars in the Magellanic Clouds. Specifically, for the first time, such abundances have been estimated for stars with significant rotational velocities. This extraordinary data set gives us the unique possibility to calibrate rotationally and magnetically induced mixing processes. Therefore, we have computed a grid of stellar evolution models varying in mass, initial rotational velocity and chemical composition. In our models we find that although magnetic fields generated by the Spruit-Taylor dynamo are essential to understand the internal angular momentum transport (and hence the rotational behavior), the corresponding chemical mixing must be neglected to reproduce the observations. Further we show that for low metallicities detailed initial abundances are of prime importance, as solar-scaled abundances may result in significant calibration errors.

**Keywords:** Stellar rotation, chemical composition, Main-sequence: early-type stars (O and B), Stellar properties, Stellar evolution
**PACS:** 97.10.Cv,97.10.Kc,97.10.Me,97.10.Tk,97.20.Ec

## INTRODUCTION

Rotational velocities and nitrogen abundances have been measured for a large sample of LMC stars as part of the VLT-FLAMES Survey of Massive Stars [1, 2]. These data have been used to set constraints on the efficiency of rotational induced mixing processes in our models. With these newly calibrated models we have investigated the influence of different chemical mixtures at SMC metallicity on the models.

## THE MODELS

We have calculated models using a stellar evolution code for single and binary stars [3, 4]. The models include rotation and magnetic fields. We have extended the code to account for different initial chemical compositions. For mass loss we have adopted the prescription of [5, 6].

We have compiled chemical mixtures for the Small and Large Magellanic Cloud and compared them to solar scaled mixtures based on Grevesse96 [7] and Asplund05 [8]. The LMC and SMC mixtures are based on the Asplund composition in which the amount of all metals has been decreased by 0.4 dex and 0.7 dex, respectively, and the abundances of C, N, O, Mg, Si and Fe have been set to the baseline values (C. Trundle ,private communications) summarized in Table 1.

**Table 1. Baseline abundances of C, N, O, Mg, Si and Fe used for the different chemical mixtures.**

| Mixture | C | N | O | Mg | Si | Fe |
|---|---|---|---|---|---|---|
| Grev96 | 8.55 | 7.97 | 8.87 | 7.58 | 7.55 | 7.50 |
| Aspl05 | 8.39 | 7.78 | 8.66 | 7.53 | 7.51 | 7.45 |
| LMC | 7.75 | 6.90 | 8.35 | 7.05 | 7.20 | 7.05 |
| SMC | 7.37 | 6.50 | 7.98 | 6.72 | 6.80 | 6.78 |

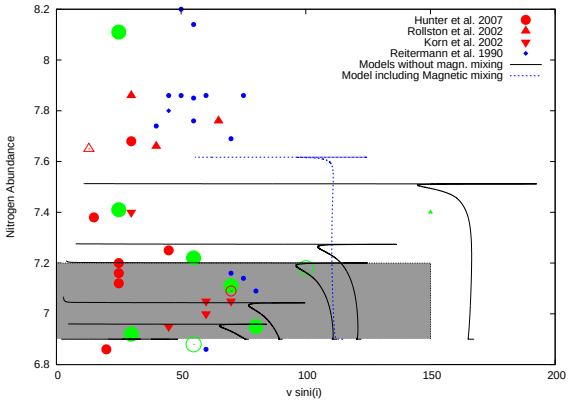


**Figure 1.** Projected surface velocity versus nitrogen abundance of LMC B-Stars. Red (middle sized), green (large sized), blue (small sized) symbols represent dwarfs ($\log g < 3.7$), giants ($3.7 \leq \log g \leq 3.2$), supergiants ($\log g < 3.2$), respectively. Open symbols represent upper limits. The gray shaded box represents the bulk of stars in [9]. Black solid lines represent models of $13 M_{\odot}$ at different initial velocities which are calibrated to fit the data of [9]. The model which is plotted with the blue dotted line takes chemical mixing processes due to magnetic fields into account.

We have used the nitrogen abundances and rotational velocities of the LMC, measured by the Flames-Survey [9, in preparation], to calibrate the chemical mixing efficiency $f_c$ for rotationally induced mixing processes [3].

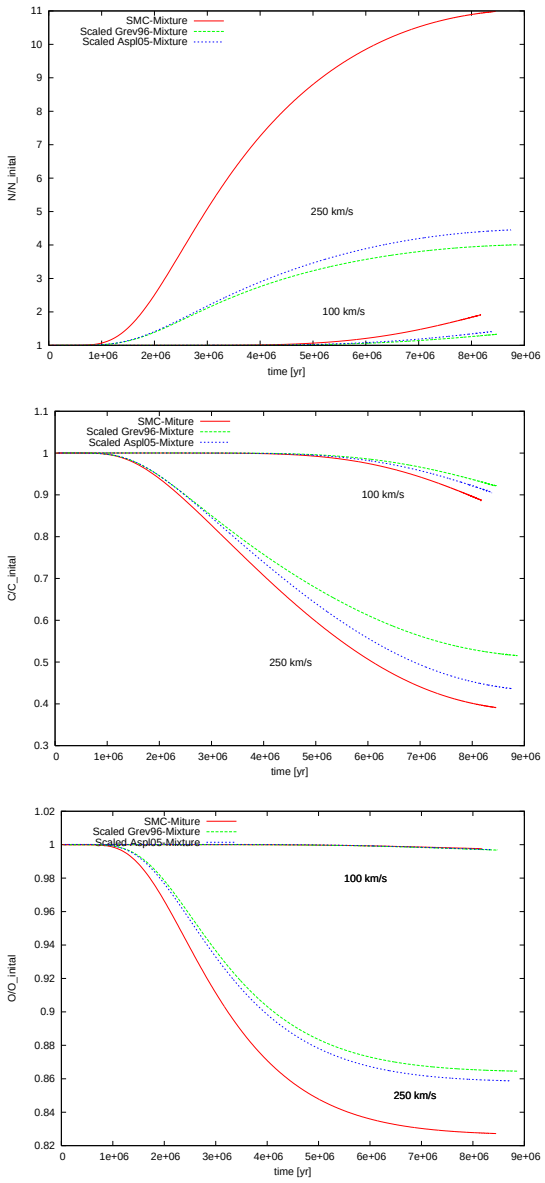


**Figure 2.** CNO surface abundance as a function of time for models with SMC mixture (red solid line) and solar-scaled SMC-Models based on the Grevesse96 mixture (green dashed line) and Asplund05 mixture (blue dotted). From top to bottom, enrichment in N, depletion in C and O for $20M_{\odot}$ models with 100 and 250 km/s initial velocity. Higher velocity results in higher enrichment/depletion.

We have used a model of $13M_{\odot}$ and an initial rotational velocity of 140 km/s (at the Zero Age Main Sequence) which agrees with the average of the sample. The chemical mixing efficiency $f_c$ has been calibrated such that the nitrogen surface abundance reached 7.2 dex at the end of the main sequence lifetime, which gave $f_c = 2.28 \cdot 10^{-2}$. The models assume an overshooting parameter of $\alpha = 0.335$, which has been adjusted to fit the observations [10].

Magnetic fields are treated as described in [11, 12]. Even though magnetic fields are needed to transport angular momentum, the efficiency for the chemical mixing must be very small. In Fig. 1, the black solid lines represent models where chemical mixing due to magnetic fields is disabled. For comparison the model which is plotted with the blue dotted line shows the nitrogen abundances reached if chemical mixing due to magnetic fields is included. The chemical diffusion process is then dominated by magnetic diffusion, resulting in too strong mixing, incompatible with the observations. The data points show data of [13] (circles), [14] (triangles), [15] (upside-down triangles) and [16] (diamonds). The grey box indicates data that will become available soon [9, in preparation].

## SOLAR-SCALED MODELS GONE BAD ?

To reproduce observed abundances and to understand how rotational induced mixing processes work in massive stars, it is of key importance to take the correct initial chemical composition into account.

To investigate the effect of the initial chemical composition, we compare the chemical enrichment/depletion of CNO in a $20\,M_{\odot}$ model at 100 and 250 km/s initial velocity and three different chemical mixtures.

Fig. 2 shows the chemical enrichment of N and the depletion in C and O during the main-sequence evolution for a SMC mixture and scaled-solar abundance patterns of Grevesse96 and Asplund05 for comparison. The solar mixtures have been scaled such that the Fe abundance is the same as for the SMC mixture. The CNO baseline abundances for the mixtures are given in

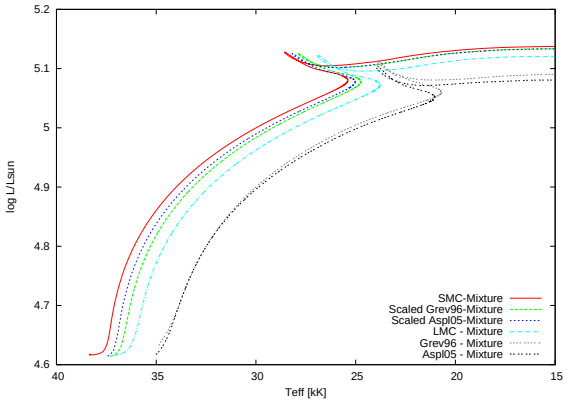


**Figure 3.** Evolutionary tracks of $20M_{\odot}$ models at 100 km/s initial velocity. The colors/line codings describe different mixtures for the initial composition used.

**Table 2.** Baseline abundances of C, N, O in SMC and Solar-Scaled-SMC Mixtures.

| Mixture | C | N | O | Fe |
|---|---|---|---|---|
| Scaled-Grev96 | 7.83 | 7.25 | 8.15 | 6.78 |
| Scaled-Aspl05 | 7.72 | 7.11 | 7.99 | 6.78 |
| SMC | 7.37 | 6.50 | 7.98 | 6.78 |

Table 2. In the case of nitrogen, the baseline abundance can differ (depending on the model) by up to 0.7 dex. The enrichment in nitrogen for the SMC mixture is about $\sim$4 times higher than for solar scaled models. For C and O the effect is less pronounced, but the depletion in C is still up to a factor 2 larger in the SMC mixture than in the solar-scaled models. We assume, the reason is the larger C/N-ratio of the SMC composition. Therefore, on the onset of the CNO cycle the model contains more carbon which can be converted into nitrogen and mixed into the bottom of the envelope before the increasing H-He gradient avoids more nitrogen leaving the core.

The HR-diagram in Fig.3 shows evolutionary tracks for a model of $20 M_{\odot}$ at 100 km/s. Shown are models (from left to right) for SMC, scaled Grevesse96, scaled Asplund05 mixtures and for comparison LMC and unscaled Grevesse96 and Asplund05 mixtures. One can see the typical shift to higher temperatures for the models with decreasing metallicity. A track using the SMC mixture is about 1 kK hotter than a comparable solar scaled model, but the temperature difference between the LMC-mixture and a solar-scaled SMC mixture is of the same order.

## CONCLUSIONS & OUTLOOK

- We find that magnetically induced instabilities give too large diffusion coefficients for chemical mixing and must, therefore, be reassessed.
- We have investigated the influence of the initial chemical composition on the models. To reproduce the correct nitrogen abundances at low metallicity and to be able to understand the ongoing mixing processes, solar-scaled initial abundances are not sufficient.
- Next we have to investigate the influence of the mixture on the opacities, as the opacity determines temperature and luminosity of the model. Currently we are using OPAL95-Tables [17], based on a Grevesse93 mixture [18].
- Rotating stars are known to show the effect of gravity darkening, which means that the poles become brighter than the equator region. The mass loss in the pole region will be therefore enhanced due to the larger luminosity, while mass loss at the equator region will be determined by rotation. Currently our models neglect this effect.

## REFERENCES


1. C. J. Evans, S. J. Smartt, J.-K. Lee, D. J. Lennon, A. Kaufer, P. L. Dufton, C. Trundle, A. Herrero, S. Simón-Díaz, A. de Koter, W.-R. Hamann, M. A. Hendry, I. Hunter, M. J. Irwin, A. J. Korn, R.-P. Kudritzki, N. Langer, M. R. Mokiem, F. Najarro, A. W. A. Pauldrach, N. Przybilla, J. Puls, R. S. I. Ryans, M. A. Urbaneja, K. A. Venn, and M. R. Villamariz, *A&A* **437**, 467–482 (2005), arXiv:astro-ph/0503655.
2. C. J. Evans, D. J. Lennon, S. J. Smartt, and C. Trundle, *A&A* **456**, 623–638 (2006), arXiv:astro-ph/0606405.
3. A. Heger, N. Langer, and S. E. Woosley, *ApJ* **528**, 368–396 (2000), arXiv:astro-ph/9904132.
4. N. Langer, *A&A* **329**, 551–558 (1998).
5. J. S. Vink, A. de Koter, and H. J. G. L. M. Lamers, *A&A* **362**, 295–309 (2000), arXiv:astro-ph/0008183.
6. J. S. Vink, A. de Koter, and H. J. G. L. M. Lamers, *A&A* **369**, 574–588 (2001), arXiv:astro-ph/0101509.
7. N. Grevesse, A. Noels, and A. J. Sauval, "Standard Abundances," in *Cosmic Abundances*, edited by S. S. Holt, and G. Sonneborn, 1996, vol. 99 of *Astronomical Society of the Pacific Conference Series*, p. 117.
8. M. Asplund, N. Grevesse, and A. J. Sauval, "The Solar Chemical Composition," in *Cosmic Abundances as Records of Stellar Evolution and Nucleosynthesis*, edited by T. G. Barnes, III, and F. N. Bash, 2005, vol. 336 of *Astronomical Society of the Pacific Conference Series*, p. 25.
9. I. Hunter, I. Brott, D. Lennon, P. Dufton, N. Langer, C. Trundle, S. Smartt, C. Evans, and R. Ryans (2007), in preparation.
10. I. Hunter, D. Lennon, P. Dufton, C. Trundle, S. Simon-Diaz, S. Smartt, R. Ryans, and C. Evans, *A&A* (2007), submitted.
11. H. C. Spruit, *A&A* **381**, 923–932 (2002), arXiv:astro-ph/0108207.
12. A. Heger, S. E. Woosley, and H. C. Spruit, *ApJ* **626**, 350–363 (2005), arXiv:astro-ph/0409422.
13. I. Hunter, P. L. Dufton, S. J. Smartt, R. S. I. Ryans, C. J. Evans, D. J. Lennon, C. Trundle, I. Hubeny, and T. Lanz, *A&A* **466**, 277–300 (2007), arXiv:astro-ph/0609710.
14. W. R. J. Rolleston, C. Trundle, and P. L. Dufton, *A&A* **396**, 53–64 (2002).
15. A. J. Korn, S. C. Keller, A. Kaufer, N. Langer, N. Przybilla, O. Stahl, and B. Wolf, *A&A* **385**, 143–151 (2002), arXiv:astro-ph/0201453.
16. A. Reitermann, O. Stahl, B. Wolf, and B. Baschek, *A&A* **234**, 109–118 (1990).
17. C. A. Iglesias, and F. J. Rogers, *ApJ* **464**, 943 (1996).
18. N. Grevesse, A. Noels, and A. J. Sauval, *A&A* **271**, 587 (1993).